NANOGRAPHITES AND THEIR COMPOUNDS

Albert M. Ziatdinov
Institute of Chemistry, Far Eastern Branch of the Russian Academy of Sciences.
Vladivostok, Russia

E-mail: albert_ziatdinov@mail.primorye.ru

Introduction

Activated carbons are representative porous materials, which have been widely used in various technologies [1]. Activated carbon fibers (ACFs), which have large specific surface areas ranging about 1000-3000 m^2g^{-1}, are microporous carbons consisting of a three dimensional disordered network of micrographites, where each micrographite has three to four graphene sheets with an average in-plane size about a few nanometers [1,2]. This particular structure makes ACFs a good model system of nanographites. There are a few reasons for an intently interest of scientists to nanographites. First, due to their intermediate position between the bulk graphite and aromatic molecules, nanographites are the potential source of new chemical substances with unusual electronic and magnetic properties. Second, while the fullerenes and carbon nanotubes are the close shaped π-electron conjugated systems [3], the electronic properties of which are mainly controlled by the quantum size and surface effects, the nanographites represent the edge-open π-electron conjugated system.

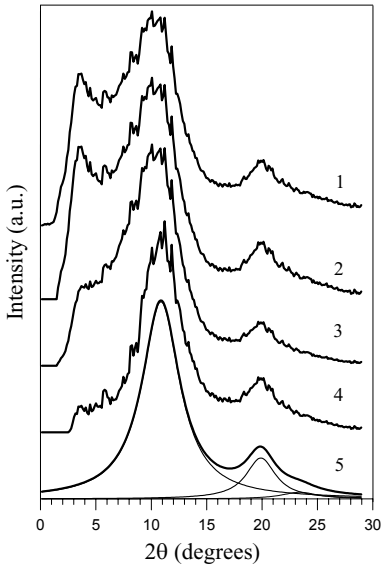

Figure 1. The X-ray diffraction spectra of ACFs. (1 – experimental; 2 – after constant background subtraction; 3 – after correction with Lorenz-polarization factor, carbon atomic form-factor and absorption factor; 4 – after angle dependant background subtraction; 5 – simulated spectrum with components, corresponding to (002), (100) and (101) peaks).

The presence of open edges around the peripheral region can result in occurrence of specific features in nanographite systems, which are different from their closed-surface counterparts [4,5]. Obviously, an arbitrary shaped graphene sheet comprises two kinds of edges: zigzag type and armchair type, while the former has a *trans*-polyacetylene type structure, while the later has a *cis*-poliacetylene type. The calculations for the model of graphite ribbons – one-dimensional graphite lattices of finite width, show that ribbons with zigzag edges possess localized edge states with energies close to the Fermi level [4,5]. These edge states correspond to the nonbonding molecular orbital (nonbonding π- levels superimposed on the bonding π and antibonding π^* bands). In contrast, edge states are completely absent for ribbons with armchair edges. However, in a general finite graphene sheet consisting of both

types of edges, even a few zigzag sites per sequence are shown to lead to non-negligible edge-state effects, resulting in an enhancement in the electronic density of states around the Fermi energy [5]. The theoretical investigations of the stacking effects in the zigzag nanographite sheets show that the edge states are sensitive to the type of the graphene layers stacking and to the interlayer interaction [6,7]. At last, it was shown that the edge states might determine the new magnetic properties in nanographene sheet, because of their relatively large contribution to the density of states at the Fermi energy [4]. The calculations show a remarkable difference in the magnetic properties between the different types of graphene layers stacking [6-8].

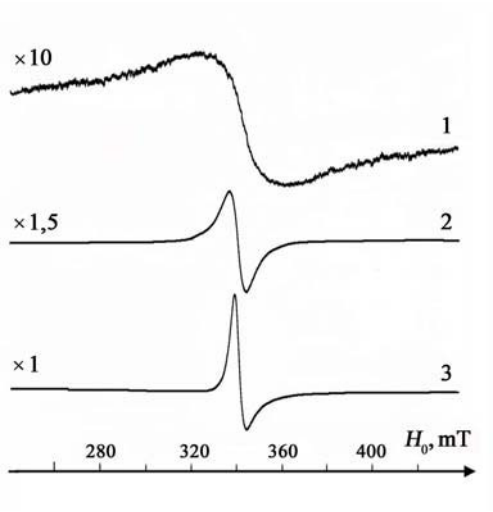

Figure 2. CESR of ACFs. (1 – initial dried up sample, 2 – sample exposed 24 hours in a water vapor and 3 – sample exposed 1 min in a liquid water).

In this paper, we present the results of X-ray diffraction, scanning tunnel microscopy, transmission electron microscopy, X-ray photoelectron spectroscopy, ESR and magnetic susceptibility study of nanographites - the structural elements (blocks) of ACFs, in order to clarify their structure and electronic properties.

Results and Discussion

The X-ray diffractograms of the ACFs show very broad peaks at the graphite (002), (100) and (101) positions, where graphite (100) and (101) peaks merge into a single broad peak around 20^0 (Fig. 1). In order to estimate the sizes of the graphite nanoparticles in ACFs, the intensities of the experimental X-ray diffractograms were corrected by standard procedures (Fig. 1). Using the corrected (002), (100) and (101) peak parameters we estimate the thickness and the in-plane size of the particle grains. From the broad graphite (002) peak, we find a grain thickness of $L_c \approx 1$ nm. We deconvulate the broad feature around 20^0-24^0 into single (100) and (101) peaks on the assumption that each peak originates mostly from a single component. The obtained contribution to the (100) peak gives an estimate of the in-plane size of $L_a \approx 2$ nm. From the location of centre for the (002) diffraction peak at $2\theta = 11.01^0$ the interlayer distance between graphene sheets are estimated at 0.375 nm, which are considerably longer than the interlayer distance of 0.3354 nm for bulk regular graphite. From nanographite sample thickness and interlayer distance between graphene sheets, the number of graphene sheets is estimated at ~3-4. The intersheet distance in nanographites reduced at the adsorption of water molecules by ACFs.

At room temperature the ESR spectrum of ACFs consists of a single line, which *g*-factor value is close to the *g*-factor value for free electron (Figs. 2 and 3b). The linewidth of signal considered depends on the amount of water molecules absorbed by ACFs and

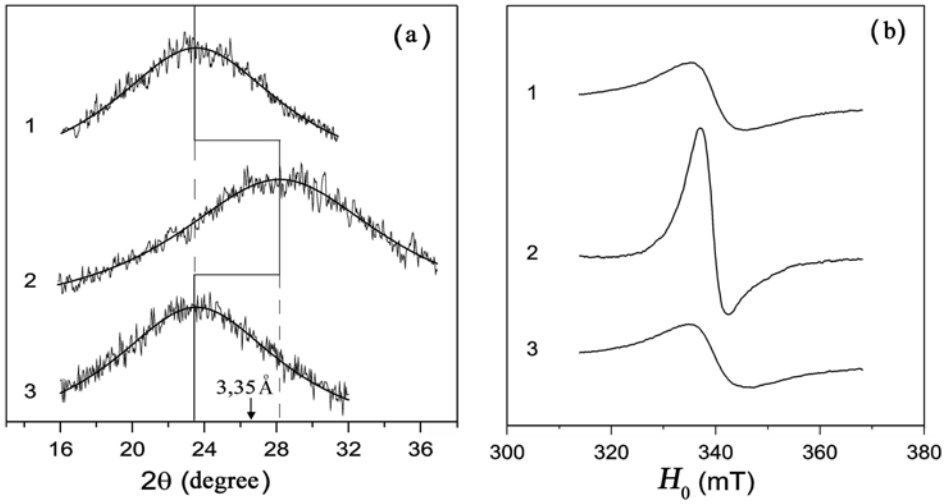

Figure 3. The changes of (002) X-ray reflection (a) and CESR signal (b) for graphite nanoparticles – structural blocks of activated carbon fibers at absorption and desorption of water molecules. (1 – initial sample, 2 – sample after adsorption of water and 3 – sample after desorption of water).

varies from ~40 mT in the initial dried up samples up to ~5 mT in treated by liquid water samples (Fig. 2). The EPR signal is practically symmetric, that specifies a weak anisotropy of the *g*-factor. At lowering of the temperature, the linewidth of this signal increases at near the constant values of *g*-factor and integral intensity. At the temperature range lower ~150 K in spectrum the second signal appears with the peak-to-peak width ~3 mT and $g \cong 2{,}0008 \pm 0.0005$ (Fig. 4). The integral intensity of this signal follows to the Curie low.

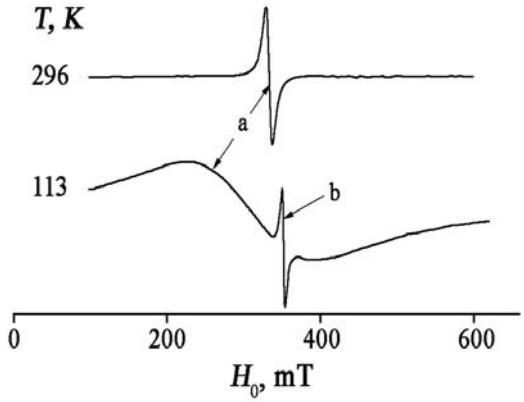

Figure 4. ESR of ACFs. (a- and b- signals of conduction electrons and localized spins, respectively).

The transformations of the (002) X-ray reflection and the CESR signal of ACFs studied at adsorption and desorption of water molecules are fully reversible (Fig. 3).

At 300 K the magnetic susceptibility is negative and equal to $(-0{,}560 \pm 0{,}001) \times 10^{-6}$ emu/g (Fig. 5). At the lowering of temperature up to 240 K it is insignificant ($\sim 0{,}4 \times 10^{-7}$) decreases, then starts to grow monotonously. At T~21 K it is near zero. At temperatures lower ~60 K a susceptibility is well described by the Curie-Weiss law with the Curie constant *(C)* and the Weiss temperature (Θ) equal to $(1{,}318 \pm 0{,}003) \times 10^{-5}$ emu·K/g and $-0{,}90 \pm 0{,}05$ K, respectively. To this Curie constant the localized spins concentration $N_s = 4 \times 10^{-3}$ spin/(carbon atom) are correspond.

Negative value of Weiss temperature specifies that between the localized spins a weak antiferromagnetic interaction present.

At the analysis, the full susceptibility was considered as the sum of core diamagnetism, Curie paramagnetism, orbital diamagnetism, and Pauli paramagnetism:

$$\chi=\chi_{core}+\chi_{Curie}+\chi_{orbital}+\chi_{Pauli},$$

where from the Pascal low $\chi_{core}= -0.5\times10^{-6}$ emu/g.

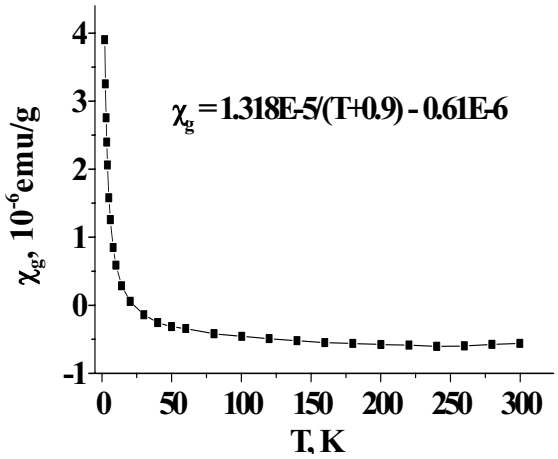

Figure 5. The magnetic susceptibility as a function of temperature for the activated carbon fibers under a magnetic field of H_0 = 0.5 T.

Taking into consideration that the interlayer distance in nanographites is significantly larger than in regular bulk graphite the former was considered to consist of finite-size non-interacting graphene sheets. To determine the value of orbital diamagnetism in nanographites the McClure [9] model of orbital diamagnetism for two-dimensional graphite, which was modified by including the Dingle temperature (the Kotosonov [10] method) was used. Thus, it was supposed that π-electrons are scattered mainly around graphene boundaries. Then, by knowing the values of χ_{core}, χ_{Curie} and the calculated value of $\chi_{orbital}$ the value of χ_{Pauli} was determined. The value of χ_{Pauli} determined by such a way and from ESR data at 113 K (Fig. 4) are one and more orders of magnitude larger than the Pauli contribution expected for bulk regular graphite for typical Fermi level energies $E_F< 0.1$ eV [11]. This results means that the density of states at the Fermi level considerably large than that in bulk regular graphite. The reasons of this may be the presence of an additional band superimposed upon the ordinary graphene bands around the Fermi level that was proposed theoretically [4,5]. Another reason of considered phenomenon is the deeper position of Fermi level in nanographite, than that in bulk regular graphite. Such displacement of the Fermi level in nanographites may be as the result of interaction of surface carbon atoms with some adsorbed molecules, such as oxygen. We shall note, that in acceptor graphite intercalation compounds a similar situation are realized and the value of displacement of the Fermi level may be significant [11]. Obviously, at the validity of the model considered, the position of the Fermi level in nanographites (as well as the sign and the value of charge on graphene layers) may be controlled by adsorption on their surface of different molecules.

As it was pointed above, in ACFs studied the intersheet distance in nanographites reduced at the adsorption by fibers of water molecules. The one of possible reason for this is the large internal pressure of water molecules adsorbed on nanographite surface, because water in the porosity of ACFs has a solid-phase structure with less density than that in the normal conditions [12]. It is obviously that the decrease of positive charge of

graphene layers as a result of donating of electrons by the adsorbed water molecules may be the another reason for this phenomenon.

Conclusions

The structure and electronic properties of nanographites - the structural elements (blocks) of activated carbon fibers were investigated by different physical methods (X-ray diffraction, scanning tunnel microscopy, transmission electron microscopy, X-ray photoelectron spectroscopy, ESR and magnetic susceptibility). The considerable enhancements of the intersheet distance and the density of states at the Fermi level were found. The conclusion was made that the reasons of this may be the presence of an additional band superimposed upon the ordinary graphene bands around the Fermi level that was proposed theoretically [4,5] or the deeper position of Fermi level in nanographite, than that in bulk regular graphite. The reversible changes of intersheet distance and CESR line shape at absorption of water molecules by ACFs was found.

Acknowledgments. The author is grateful to V.V. Kainara, Yu.M. Nikolenko and V.V. Ikorskii for help in experiments and to P.G. Skrylnik for help in calculations. This work was supported by the Russian Foundation for Basic Research (grant No. 04-03-32135) and by the Program of Basic Research of the Russian Academy Science Presidium (The Basic Problems of Physics and Chemistry of Nanosized Systems and Nanomaterials).

References

[1] Marsh H. Activated carbon compendium. Amsterdam: Elsevier Science, 2001. 300 p.
[2] Kaneko K, Ishii C, Kanoh H, Hanzawa Y, Setoyama N and Suzuki T. Characterization of porous carbons with high resolution α_s–analysis and low temperature magnetic susceptibility. Adv. Colloid Interface Sci. 1998;**76-77**:295-320.
[3] Dresselhaus MS, Dresselhaus G. and Eklund PC. Science of Fullerenes and Carbon Nanotubes. San Diego: Academic, 1996. 260 p.
[4] Fujita M, Wakabayashi K, Nakada K and Kusakabe K. Peculiar localized state at zigzag graphite edge. J. Phys. Soc. Jpn. 1996;**65**:1920-1923.
[5] Nakada K, Fujita M, Dresselhaus G and Dresselhaus MS. Edge state in grapheme ribbons: nanometer size effect and edge shape dependence. Phys. Rev. 1996;B**54**:17954-17961.
[6] Harigaya K. Mechanism of magnetism in stacked nanographite. J. Phys.: Condens. Matter 2001;**13**:1295-1302.
[7] Harigaya K and Enoki T. Mechanism of magnetism in stacked nanographite with open shell electrons. Chem. Phys. Lett. 2002;**351**:128-134.
[8] Shyu FL and Lin MF. Electronic properties of AA-stacked nanographite ribbons. Physica 2003;E **16**:214-222.
[9] McClure JW. Diamagnetism of graphite. Phys. Rev. 1956;**104**:666-671.
[10] Kotosonov AS. Diamagnetism of quasi-two-dimensional graphites. JETP Letters 1986;**43**(1):37-39.
[11] Dresselhaus MS and Dresselhaus G. Intercalation compounds of graphite. Adv. Phys. 1981;**30**:139-326.
[12] Alcaniz-Monge J, Linares-Solano A and Rand B. Mechanism of adsorption of water in carbon micropores as revealed by a study of activated carbon fibers. J. Phys. Chem. 2002;B**106**:3209-3215.